Simulations of the Hydrological Cycle over Southern South America Using the CPTEC/COLA AGCM

DANIEL ANDRÉS RODRIGUEZ AND IRACEMA F. ALBUQUERQUE CAVALCANTI

Centro de Previsão de Tempo e Estudos Climáticos, Instituto Nacional de Pesquisas Espaciais, Cachoeira Paulista, Brazil

(Manuscript received 10 January 2005, in final form 18 January 2006)

ABSTRACT

The La Plata River basin is the second largest basin of South America after the Amazon basin, and it is located in an international area that occupies territories of Argentina, Uruguay, Brazil, Paraguay, and Bolivia, areas of great economic activity. In the present work, the water budget over the region was studied and the atmospheric and terrestrial components were analyzed to investigate the Center for Weather Forecast and Climate Studies/Center for Ocean–Land–Atmosphere Studies (CPTEC/COLA) atmospheric general circulation model (AGCM) behavior in a simulation of 10 yr. The analysis was performed considering two sectors, northern and southern, because of their different behaviors, and the main characteristics were simulated by the model. The northern sector presents a well-defined annual cycle with well-established wet conditions in the summer, when there is development of the South Atlantic convergence zone (SACZ). In the southern sector, there is a weak annual cycle and the hydrological variables do not have large seasonal variations as in the northern sector. A period of maximum precipitation is identified at the end of spring in the southern sector. Moisture flux convergence (MFC) in the model occurs over southeast Brazil during summer and over northern Argentina in the spring, consistent with observations. Analysis of the meridional and zonal moisture fluxes reveals that there is an intrusion of moisture from the tropical region, southward, and also flux from the Atlantic Ocean, that feed both sectors. The flux from the Amazon region was the main source of external moisture during the summer season, while the flux from the Atlantic Ocean was dominant during winter. Additional analysis of El Niño 1982/83 and La Niña 1988/89 episodes showed the importance of Amazon and Atlantic moisture fluxes to the La Plata basin region. During El Niño 1982/83 there was more moisture flux from the Amazon region to the southern sector than during La Niña 1988/89. This feature was related to droughts during La Niña and floods during El Niño in the La Plata region.

1. Introduction

The hydrological cycle has a large importance on climate studies due to the interaction existing between the land and the atmosphere through energy, water, and momentum exchanges, as well as photosynthetic processes (O'Kane 1994; Harding and Jochum 1995). In South America, besides the Amazon basin in the tropical region, there is another large basin, the La Plata basin, which is located in the southeastern region of South America (SSA). This basin, with 3 100 000 km^2, comprises territories with great economic activity of Argentina, Uruguay, Brazil, Paraguay, and Bolivia (Garcia and Vargas 1996). In general, waters flow from north to south and the surface hydrology is basically influenced by the topography. Toward the eastern side, the basin has average heights of 1000 m, varying from 1500 m at the Brazilian plateau to 200 m at the Argentinean pampas. The Andes Cordillera is located on the western side of the basin with heights between 1000 and 4000 m. Mean annual river discharge in the extreme south of the La Plata basin is about 21 000 m^3 s^{-1}. This amount results from the contribution of the three main tributaries, the Paraná River, Paraguay River, and Uruguay River. The Paraná River has a discharge of approximately 17 700 m^3 s^{-1}, which includes the Paraguay River discharge of 2700 m^3 s^{-1}, and the Uruguay River discharge is 4000 m^3 s^{-1} (Garcia and Vargas 1996).

The annual average rainfall presents a maximum value of 1800 mm toward the Brazilian coast and decreases southward and westward. The northern and southern regions of the La Plata basin display different behavior regarding the annual cycle of precipitation

Corresponding author address: Daniel Andrés Rodriguez, CPTEC/INPE, Rod. Presidente Dutra, Km. 40, Cachoeira Paulista, S.P., Brazil.
E-mail: dandres@cptec.inpe.br

(Berbery and Barros 2002). The northern regime is associated with the South American monsoon system and is affected by the South Atlantic convergence zone (SACZ), which is identified as a persistent northwest–southeast strong convection cloud band (Kodama 1992). On the other hand, the southern region of the basin is affected during the whole year by frontal systems and by cyclonic vortices at upper levels, which are responsible for part of the observed precipitation (Satyamurty et al. 1998). In addition, during spring and summer, mesoscale convective complexes (MCCs) develop in the southern sector causing intense precipitation in the area (Velasco and Fritsch 1987). Maximum precipitation occurs during the night, and the MCCs have been connected to the occurrence of a low-level jet (LLJ) east of the Andes Cordillera (Velasco and Fritsch 1987; Nicolini et al. 2002).

The moisture transport by the LLJ from the Tropics to the high latitudes over the continent was first discussed by Virji (1981), who used satellite estimates of low-level winds. The effect of this LLJ on the water vapor transport over SSA was studied by Berri and Inzunza (1993), using station data and results of a mesoscale model simulation. The nocturnal maximum of the LLJ was related to the springtime nocturnal maximum in precipitation over the central part of La Plata basin in studies with the regional Eta Model (Berbery and Collini 2000). On the other hand, the daytime maximum of precipitation over southern Brazil was related to the thermodynamic environmental conditions that induce the growth of convective available potential energy. Two diurnal regimes were found to modulate the atmospheric hydrological cycle of the La Plata basin (Berbery and Collini 2000). Unlike many LLJs around the world, the one east of the Andes is present throughout the year (Berbery and Barros 2002) and contributes to the moisture budget in the basin, even during the cold season. The recent development of the South American Low-Level Jet Experiment (SALLJEX) is leading to several new articles that are expected to reveal more features of this LLJ (Vera 2004). One particular area of interest is whether, and to what extent, the jet and its relation to precipitation can be predictable.

A previous study of moisture transport and the hydrological cycle over South America, from a global analyses dataset, can be found in Rao et al. (1996). In that study, a high content of water vapor over the SACZ in the southeast of Brazil and over the Amazon was found and the importance of the Atlantic Ocean as a source of moisture for the Amazon basin was discussed. Labraga et al. (2000) tried to link the cycle of water vapor with the circulation in the troposphere over South America. The authors found that the stationary water vapor flux convergence plays an important role in producing the maxima rainfall rate over the southeastern part of South America and the SACZ during summer. Studies of LLJ features were developed by Saulo et al. (2000) using the regional Eta Model. In that analysis, a moisture convergence pattern to the south of 20°S was related to a north–south main component of water vapor flux at low levels from the Amazon region to SSA during spring and summer of the El Niño year 1997/98. Saulo et al. (2000) identified two sources of moisture for the region during the 1997/98 warm season. The southward flux originated in tropical South America, which was found to be the dominant source, and the northeasterly flux from the South Atlantic anticyclone.

GCM simulations of the water budget of the Amazonian basin have been analyzed in several studies, including Marengo et al. (1998), Zeng (1999), Costa and Foley (1999), and many others. However, studies on the La Plata basin have been performed mainly with regional models, as in Berbery and Collini (2000) and Saulo et al. (2000). The Center for Weather Forecast and Climate Studies (CPTEC) uses an atmospheric general circulation model (AGCM) for weather forecasts, seasonal prediction, and simulation experiments. Climatological and seasonal results using this model are documented in Cavalcanti et al. (2002a). The model simulates well the main seasonal characteristics over the globe associated with atmospheric variables and precipitation. However there is an overestimation of precipitation over the southern part of the SACZ and over the Andes Cordillera, and an underestimation over Amazon and over southern Brazil, Paraguay, Uruguay, and Argentina (Cavalcanti et al. 2002a). Systematic errors identified in those climatic simulations were mainly related to physical parameterizations, such as convection and radiation schemes.

Results of seasonal prediction performed at CPTEC with the CPTEC/Center for Ocean–Land–Atmosphere Studies (COLA) AGCM (Cavalcanti et al. 2000) have been used to provide rainfall advisories and have benefited several sectors, including the agriculture, hydroelectric power, and social sectors that are in the La Plata basin region. The model rainfall is a component of the hydrological cycle that should be well simulated for climate study purposes. A difficulty in the hydrological cycle modeling, using climate and weather models, consists in the incorporation of land interface processes and their feedbacks. There are models in which the treatment of these processes are performed with complex modules, like the Simplified Simple Biosphere Model (SSiB; Xue et al. 1991), used in the CPTEC

COLA AGCM. The main source of model uncertainties in weather and climate simulations is related to the hydrological cycle (O'Kane 1994). In addition, Wang and Paegle (1996) show that there are differences between the moisture budgets obtained with analysis from different datasets [European Centre for Medium-Range Weather Forecasts (ECMWF), U.S. National Centers for Environmental Prediction, and U.K. Met Office]. The sources of error result from model surface elevation fields, gaps in the data archive, and uncertainties in the wind and specific humidity analyses, even though a discussion of the model results on the hydrological cycle over the La Plata basin is required in order to verify the model behavior in the region, and to discuss features of the simulated atmospheric flow and sources of moisture flux.

The objective of this study is to examine the annual cycle climatology and interannual variability of the hydrological cycle over SSA simulated by the CPTEC/COLA AGCM and to examine what the moisture sources for precipitation over the La Plata basin are. It is intended to show the importance of these sources for SSA climatology and their interannual variability by studying the warm seasons of two extreme ENSO events (1982/83 and 1988/89). Section 2 describes the data and the methodology utilized. In section 3, climatological features of the hydrological cycle are discussed, considering the northern and southern sectors of the La Plata basin, including the relations between the seasonal variability of the low-level atmospheric flow and the zonal and meridional moisture flux into the sectors. Analyses of El Niño 1982/83 and La Niña 1988/89 events are shown in section 4, and conclusions are drawn in section 5.

2. Data and methodology

The study was developed using results of an ensemble of nine integrations performed for 10 yr (1982–91) using the CPTEC/COLA AGCM with horizontal triangular resolution of 62 waves and 28 vertical levels (T62L28). This model is a modified version of the spectral COLA AGCM, which is described in Kinter et al. (1997). It has a land surface module, the SSiB (Xue et al. 1991), which takes into account "the selective absorption of photosynthetically active radiation; the root and stomatal resistance to water vapor fluxes from the soil to the atmosphere; the storage, drainage and evaporation of intercepted precipitation and dew from plant surfaces; the runoff of excess precipitation and drainage of ground water; the thermal and radiative effects of snow cover on the ground and canopy surface; the influence of different plant morphologies on roughness length, and hence transfer to momentum, heat and moisture between land and atmosphere" (Kinter et al. 1997).

The simulation was performed considering consecutive days as initial conditions, from 11 to 19 September 1981, which were obtained from ECMWF daily analyses. The monthly observed sea surface temperatures (SSTs) from the Climate Prediction Center/National Centers for Environmental Prediction (CPC/NCEP) monthly optimum interpolation SST dataset (Reynolds and Smith 1994) were applied as forcing boundary conditions. The model description and discussion of systematic errors obtained from this climate simulation are reported in Cavalcanti et al. (2002a).

The observed precipitations were extracted from the Climatic Research Unit (CRU) and CPC Merged Analysis of Precipitation (CMAP) datasets. The resolution of the CRU precipitation dataset is $0.5° \times 0.5°$ and was constructed using information of stations over land. It was used by New et al. (1999, 2000) to develop a monthly climatology over the globe. The resolution of the CMAP dataset is $2.5° \times 2.5°$ and was constructed merging information from stations with several satellite estimations. A description of this dataset can be found in Xie and Arkin (1996, 1997).

Atmospheric features were discussed based on variables from the NCEP–Department of Energy (DOE) reanalysis II (R2) (Kanamitsu et al. 2002) for the same period of the CPTEC/COLA integration. It is believed the R2 dataset estimates the water-related elements more accurately in tropical and also in middle and high latitudes. R2 used an updated version of the NCEP medium-range forecast (1999 NCEP MRF) of the original global spectral model (GSM), fixing a number of bugs in the earlier reanalysis and changing physical parameterizations. A new scheme derived from the two-layer soil model of Pan (1990) was incorporated at the land surface parameterization to replace the former bucket model. In addition, the treatment of soil moisture was changed from the NCEP–National Center for Atmospheric Research (NCAR) reanalysis (Kalnay et al. 1996). A correction based on the difference between observed and simulated precipitation was incorporated to simulate soil moisture. Roads et al. (2002) developed a detailed study about water and energy budgets from R2, and showed the existence of artificial residual forcings in both budgets. These residuals are implicitly included, in order to force the state variables to values close to observations and provide an estimate of the overall error in the budgets (Roads et al. 2002). It is important to note that the evapotranspiration from R2 is a calculated variable rather than an observed one. It is obtained using the reanalysis II model and could introduce some errors in the budget analysis, although

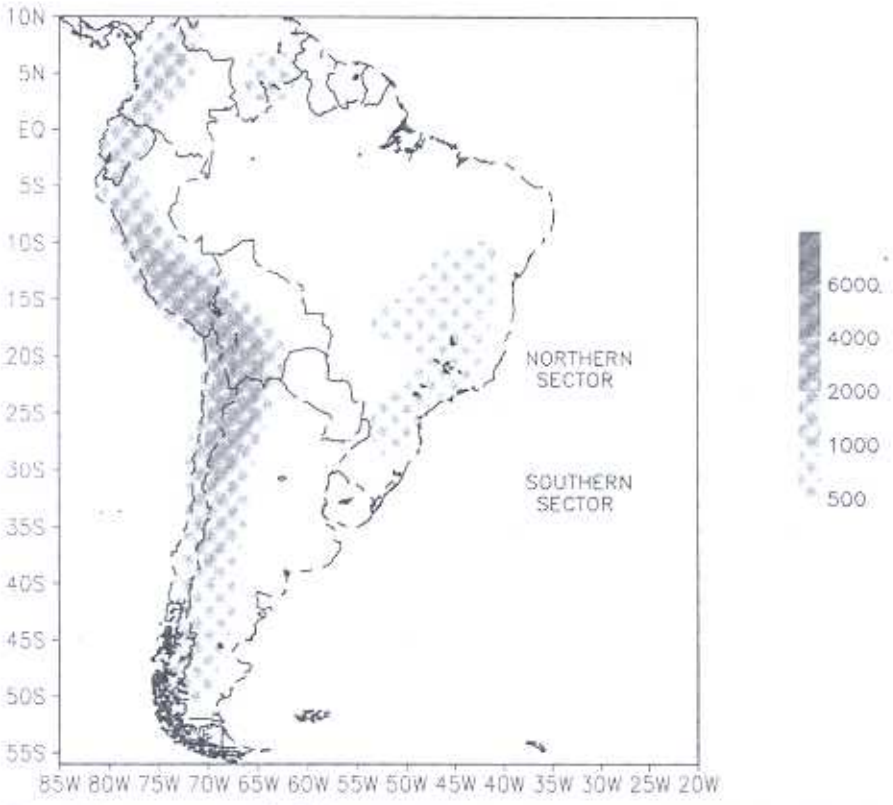

FIG. 1. Northern sector (15°–25°S, 64°–40°W) and southern sector (25°–40°S, 64°–40°W) of La Plata basin in South America. Topography is in meters.

fewer errors than if the previous reanalysis was considered. Meanwhile, in the present study, this variable is used to address the R2 budget and compare with the model budget rather than to validate the CPTEC/COLA simulations of evapotranspiration.

In the present study, the diagnostics were performed considering the seasonal climatology, and also the spring and summer of El Niño 1982/83 and La Niña 1988/89 events. During these seasons the MCCs are frequent over the La Plata basin region, and account for a large part of the total precipitation (Velasco and Fritsch 1987; Laing and Fritsch 2000), and during summer there is also high convective activity over tropical South America. To analyze the hydrological balance over SSA, the region was separated in two sectors, northern and southern, based on their different precipitation regimes. The spatial averages were calculated only over the continental area. The northern sector comprises the area between 15°–25°S and 64°–40°W, which is influenced by a tropical regime and is affected by the SACZ in the summer. The southern sector is the area of 25°–40°S, 64°–40°W, which has an extratropical regime (Fig. 1). The water budget analysis was restricted to these two regions, although the atmospheric circulation was analyzed over the whole South America.

The water balance was performed following the method discussed by Peixoto and Oort (1992), using the simplifications of Rasmusson (1967) and Roads et al. (1994). Then, for areas larger than 20×10^5 km^2 and when temporal ($^-$) and spatial ([]) averages are considered, the land component is described in Eq. (1) and the atmospheric component in Eq. (2):

$$[\bar{P} - \bar{E}] = \left[\frac{\partial S_m}{\partial t}\right] + [\bar{R}_0], \tag{1}$$

$$[\bar{E} - \bar{P}] = \left[\frac{\partial \bar{W}}{\partial t}\right] + [\nabla \cdot \bar{Q}], \tag{2}$$

where P is the time-averaged precipitation, E is the time-averaged evapotranspiration, R_0 is the time-averaged direct runoff, $\bar{Q}$ is the time-averaged moisture flux, $\bar{W}$ is the moisture storage in the atmosphere, and S_m is the moisture storage into the soil. For long-term averages and large areas both first terms in the right-hand sides of Eqs. (1) and (2) tend to be small compared to the others terms (Peixoto and Oort 1992) and they can be neglected.

The moisture flux was integrated vertically and over the lateral contours of the northern and southern sector to evaluate the input and output of moisture in these areas (Fig. 1). The equations are

$$Q_{\phi_1} = \int_{\lambda_1}^{\lambda_2}\int_{p_0}^{p}\frac{qv}{g}\,dp\,d\lambda\Bigg|_{\phi_1} \quad Q_{\phi_2} = \int_{\lambda_1}^{\lambda_2}\int_{p_0}^{p}\frac{qv}{g}\,dp\,d\lambda\Bigg|_{\phi_2}$$
$$Q_{\lambda_1} = \int_{\phi_1}^{\phi_2}\int_{p_0}^{p}\frac{qu}{g}\,dp\,d\phi\Bigg|_{\lambda_1} \quad Q_{\lambda_2} = \int_{\phi_1}^{\phi_2}\int_{p_0}^{p}\frac{qu}{g}\,dp\,d\phi\Bigg|_{\lambda_2}, \tag{3}$$

where Q_ϕ is the vertically integrated moisture flux through latitude ϕ, Q_λ is the vertically integrated moisture flux through longitude λ, q is the specific moisture, and (u, v) are the wind components. The integration was performed between a surface pressure level p_0 and the pressure level p (300 hPa).

The temporal evolution of the area averages (over land) of soil moisture, runoff, rainfall, moisture flux convergence, and evapotranspiration was analyzed to detect their interrelations during different months of the year. The water balance was calculated utilizing spatial average values of the north and south sectors separately. The same analyses were made considering El Niño 1982/83 and La Niña 1988/89 spring and summer.

The difference $P - E$ over the two sectors was analyzed to verify moisture sources or sinks (Lau et al. 1996). The evolution of $P - E$ was studied along with evolutions in runoff and soil moisture in order to analyze recharge and drainage stages (Bonan 1998; Betts et al. 1998). The evapotranspiration was also related to the previous analysis in order to show how the soil water affects the evaporation's maintenance (Bonan 1998; Betts and Viterbo 2000; Roads and Betts 2000). Comparing the $P - E$ values with the moisture convergence and with the runoff, the adjustment in the water balance over the region was analyzed. Moisture convergence values were compared with evapotranspiration estimates to assess the relative importance between internal and external moisture sources.

3. Climatological features

a. Seasonal variability

The climatological seasonal precipitation simulated by the model, observed CRU, and the difference fields over SSA are shown in Fig. 2. CPTEC/COLA overestimates precipitation over the northern sector and underestimates it over the southern sector. The overestimation is seen mainly in the area of the SACZ, a system that can occur from late spring to summer and early autumn. Large differences between simulated and observed precipitation are found mainly during summer, followed by spring and fall. Similar behavior is found when compared with the precipitation from CMAP (not shown). The overestimation in the SACZ area noticed in CPTEC/COLA AGCM results has been related to the convection parameterization scheme by Cavalcanti et al. (2002a). The convection parameterization is the Kuo scheme (Kuo 1974), based on large-scale moisture convergence. In the seasonal analysis it is seen that there is also overestimated precipitation in the SACZ area in the winter, although there is not occurrence of this system in this season. The overestimation could be related to errors in the conversion of moisture convergence to precipitation. The high precipitation values observed over the southern sector during autumn and winter were not represented by the model.

According to Fig. 3, the global R2 moisture flux shows divergence over the eastern area of the northern sector in winter and also in autumn. Model results show convergence, and thus the difference fields show an excess of convergence over the southeastern coast of Brazil, even during the winter dry season. In summer and spring, moisture convergence follows the precipitation maximum and there is excess of moisture convergence in model simulations. Although less than observed, moisture convergence is estimated by CPTEC/COLA over the southern sector in all seasons, as in R2 (Fig. 3). In the spring the maximum of moisture convergence is reasonably well simulated. This is the season when differences between model estimations and observed precipitation are small over the southern sector.

Comparing precipitation patterns from the model and from observations with model and R2 moisture convergence, it is seen that, although there are systematic errors, the CPTEC/COLA model represents the convergence fields more accurately than precipitation fields. This finding suggests that the occurrence of errors in precipitation could be partly associated with limitations of the Kuo parameterization to convective precipitation. The Kuo scheme computes precipitation from the large-scale moisture convergence, while the convective precipitation is the result of the release of potential instability and not the direct result of moisture flux convergence.

The patterns of convergence (Fig. 3) and $P - E$ (Fig. 4) are similar over the northern sector, indicating that the storage of water in the atmosphere and in the soil is negligible. In the southern sector, moisture convergence is larger than $P - E$ in summer and spring. This behavior indicates CPTEC/COLA stores moisture during these seasons. Summer and spring are the wet sea-

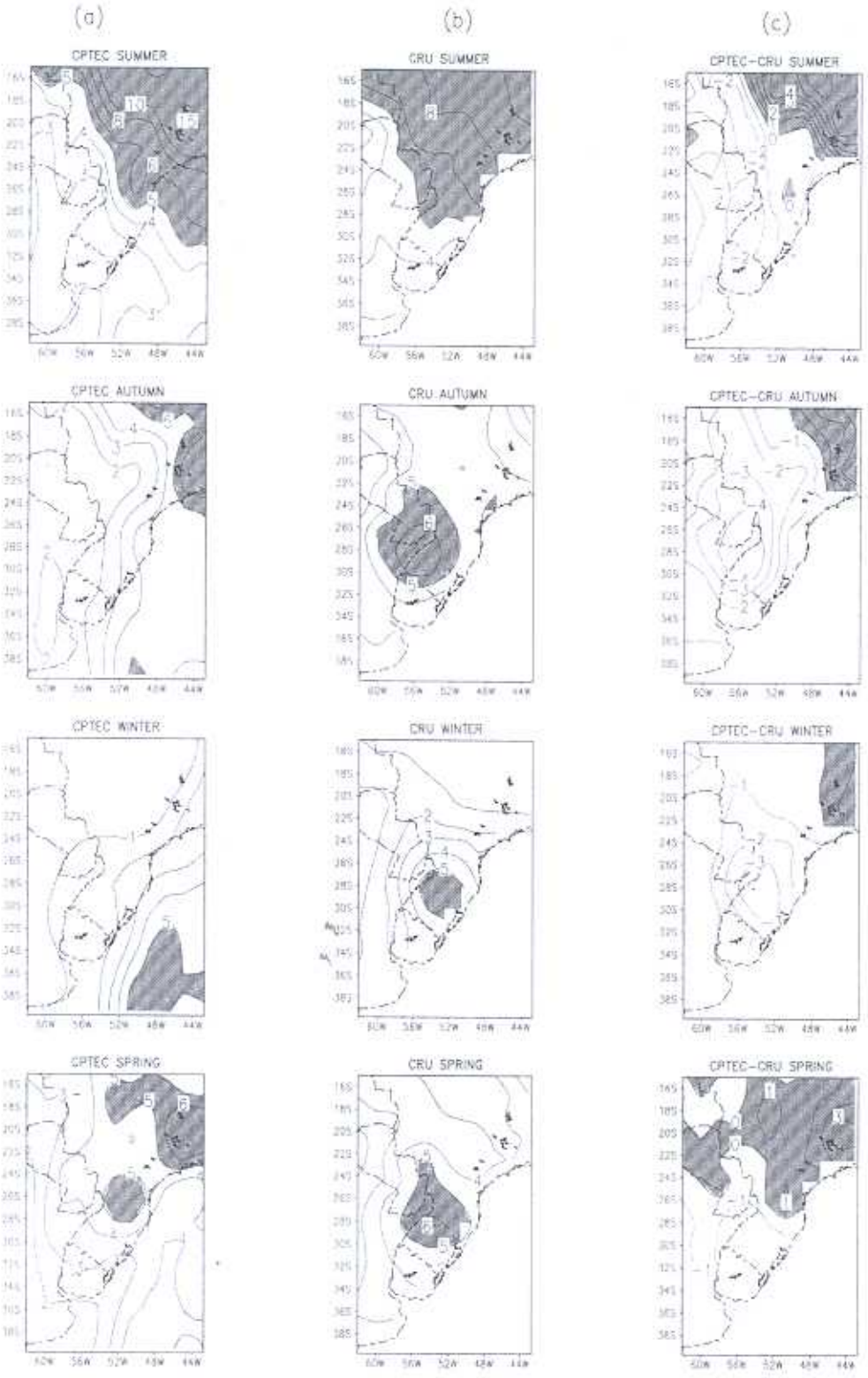

FIG. 2. Seasonal climatological precipitation (kg m^{-2} day^{-1}) from (a) CPTEC/COLA AGCM, (b) CRU, and (c) the difference between CPTEC/COLA and CRU. Values greater than 5 (kg m^{-2} day^{-1}) for the fields and positive for the differences are shaded.

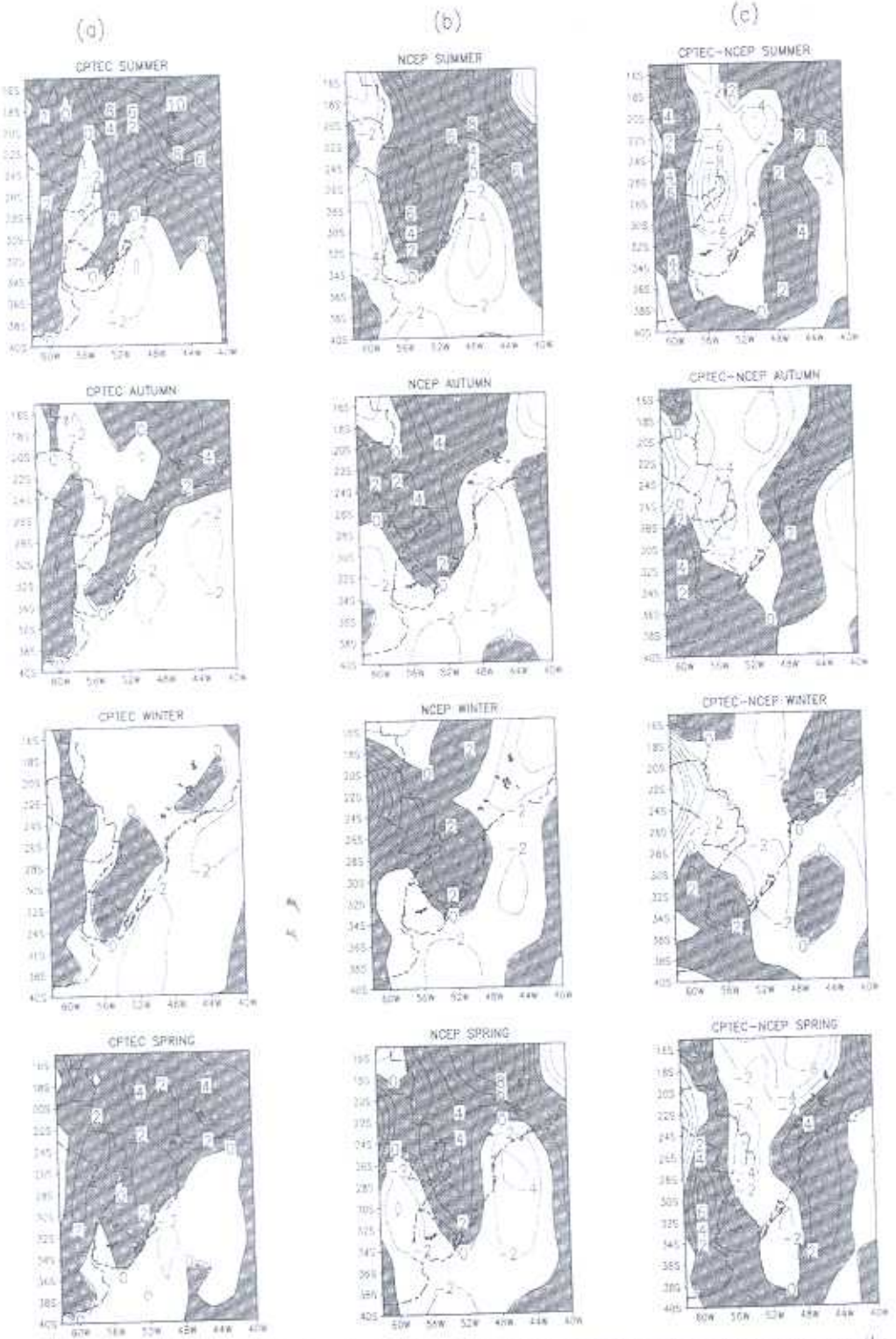

FIG. 3. Seasonal climatological vertically integrated (surface–300 hPa) moisture flux convergence (kg m^{-2} day^{-1}) from (a) CPTEC/COLA, (b) R2, and (c) the difference between the CPTEC/COLA AGCM and R2. Convergence values are shaded.

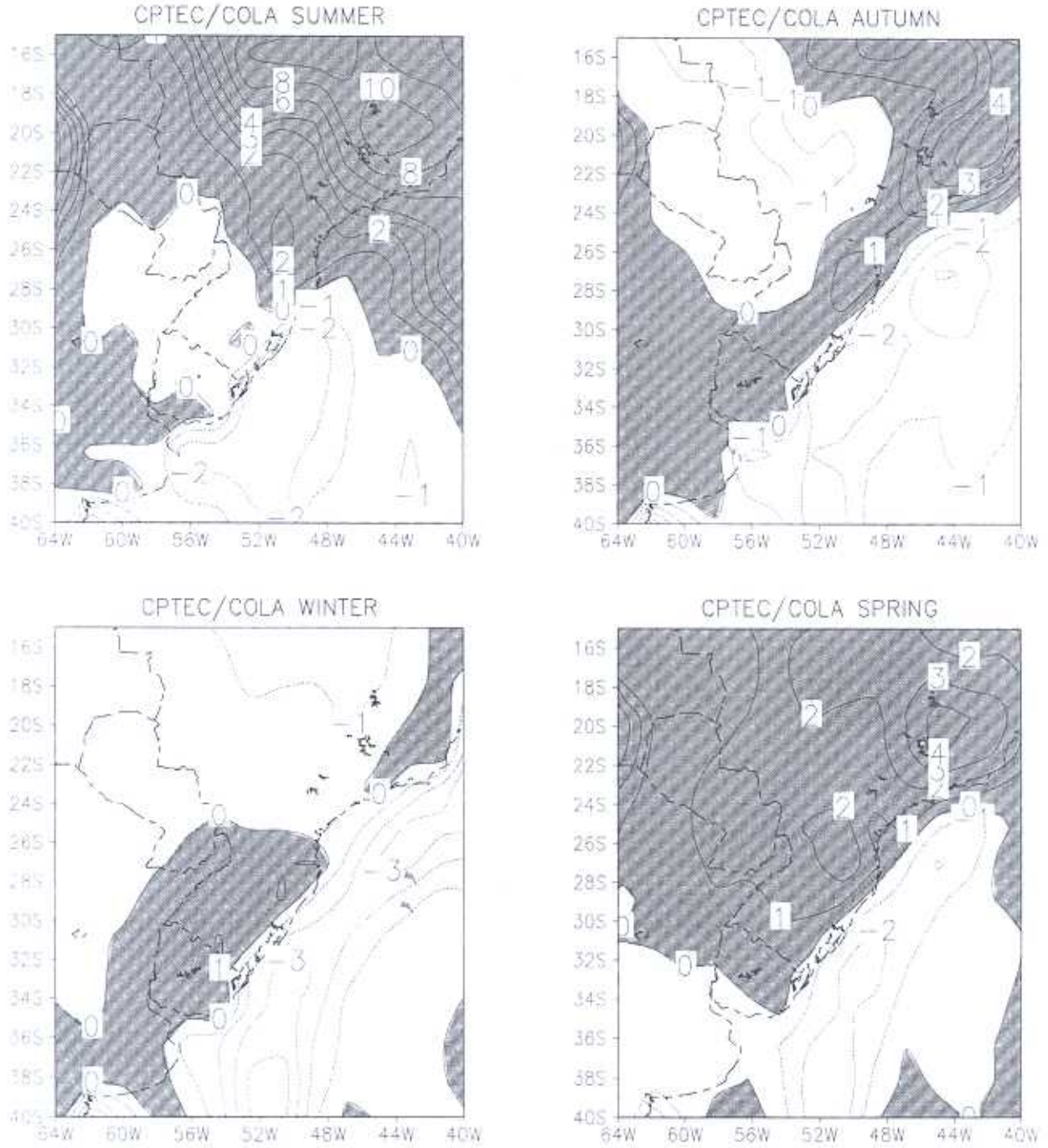

FIG. 4. Seasonal climatological precipitation – evapotranspiration (kg m^{-2} day^{-1}) from the CPTEC/COLA AGCM. Positive values are shaded.

sons in central and southeast Brazil characterized also by high convective activity over Amazonia. The unbalance between precipitation, evaporation, and moisture convergence in the southern sector during these seasons suggests that the excess of moisture is attributed to the transport of water vapor into the southern sector from the northern sector. A discussion of the moisture transport is presented in section 3c.

b. Annual cycles in northern and southern sectors

The area averages of simulated precipitation are closer to the observations in the northern than in the

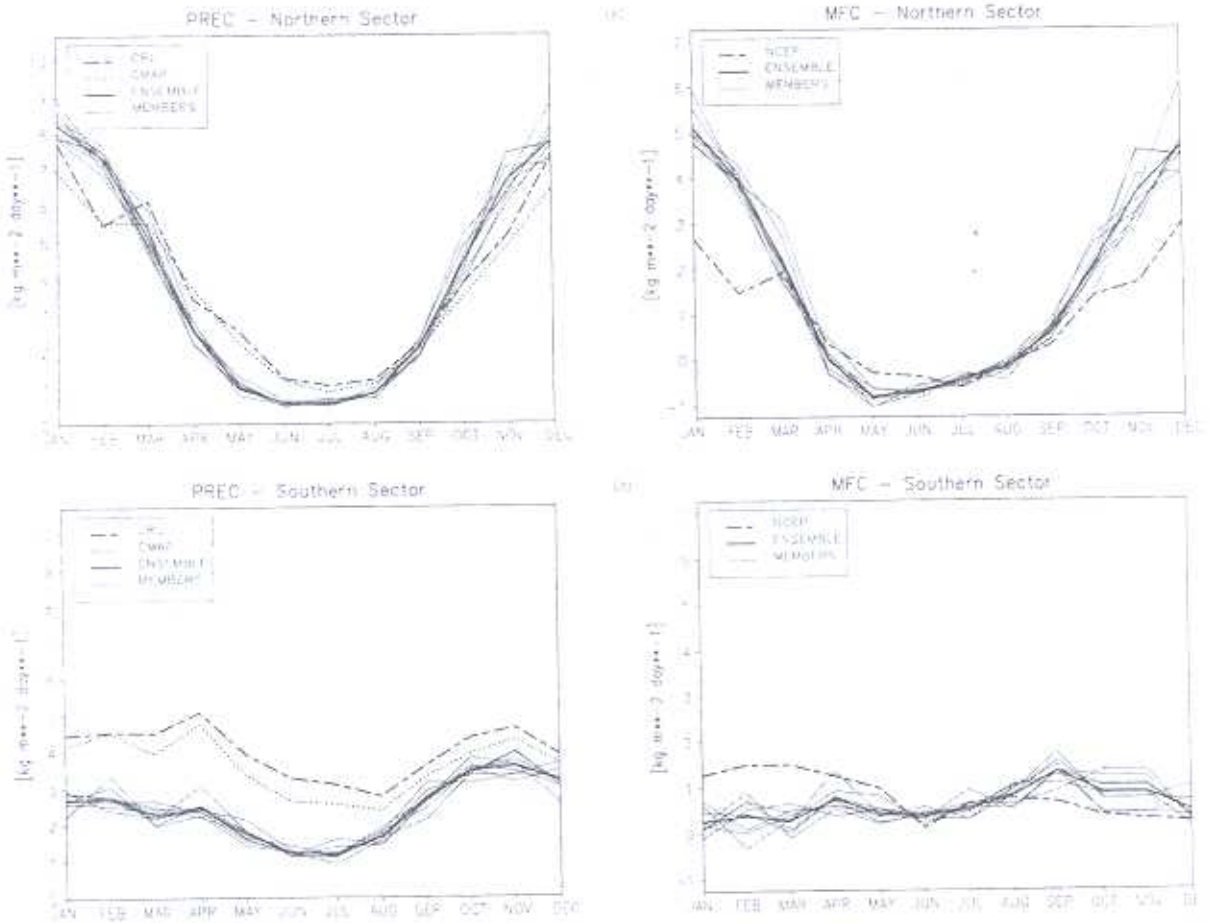

FIG. 5. Spatial averaged precipitation (P) (kg m^{-2} day^{-1}) and spatial averaged vertically integrated moisture flux convergence (MFC) (kg m^{-2} day^{-1}) in the (a), (b) northern and (c), (d) southern sectors. CPTEC/COLA ensemble members in think lines, CPTEC/COLA ensemble average in solid line, CMAP precipitation in dotted line, and CRU precipitation and R2 MFC in dashed line.

southern sector (Figs. 5a,c) where observed values are underestimated during the whole year. The precipitation over the northern sector presents a maximum in summer and late spring and a minimum in winter in agreement with both observations, CRU and CMAP. The drop of precipitation in February noticed in the observed datasets exists also in reanalysis moist convergence and it is not captured by the model. The reduction of precipitation in the northern sector in February can be related to the climatological reduction of SACZ cases that are more frequent in December and January. However, the model continues to show precipitation in February associated with the SACZ.

Over the southern sector, the annual cycle of precipitation is smoother than in the northern sector for both model and observations, and although the ensemble and members show underestimated values, the secondary maximum in spring is well represented. Analogous to the northern sector, a minimum in precipitation is found during wintertime. However, the model shows much lower than the observed precipitation from January to August. It must be noticed than in both sectors the precipitation from CRU dataset and from CMAP dataset had similar behaviors.

In the northern sector, the annual cycle of moisture convergence evolves similarly to the annual cycle of the R2 (Fig. 5b). There is overestimation of moisture convergence at the end of spring and in summer, which is consistent with the precipitation behavior. Differences between R2 and model simulation are found during some months in the southern sector, except from June through August when there is a minimum in both model and observation, and the agreement between the datasets is significantly high (Fig. 5d).

Area-averaged hydrological variables from CPTEC/COLA model results show a well defined annual cycle over the northern sector (Fig. 6a). Moisture supplied from local sources (evapotranspiration) has similar magnitude than the supply from external sources (moisture convergence) over the northern sector from the

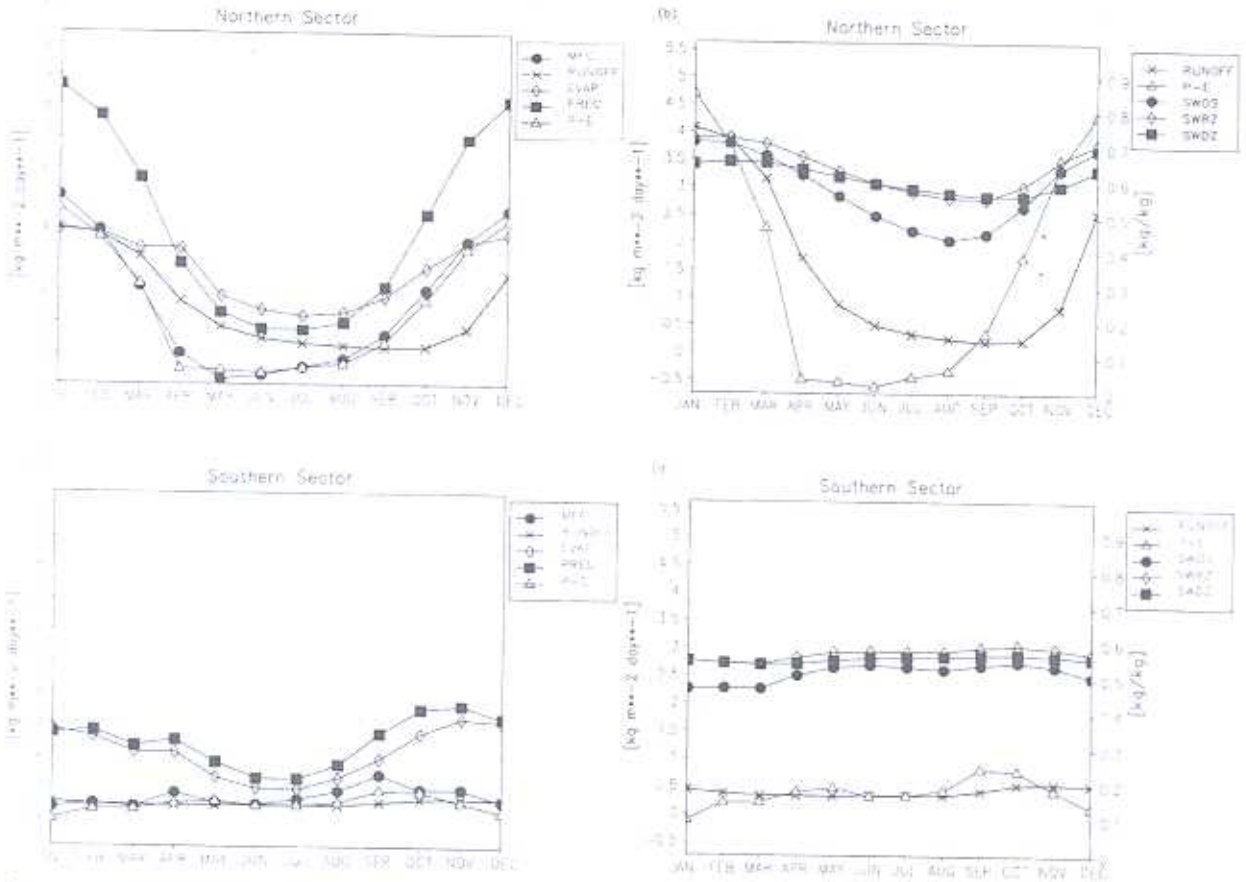

FIG. 6. Annual cycle of the spatial averaged variables of the hydrological budget over the (a), (b) northern and (c), (d) southern sectors from the CPTEC/COLA AGCM. [EVAP: Evapotranspiration (kg m^{-2} day^{-1}); PREC: Precipitation (kg m^{-2} day^{-1}); RUNOFF: Runoff (kg m^{-2} day^{-1}); MFC: vertically integrated moisture flux convergence (kg m^{-2} day^{-1}); P-E: Precipitation and evapotranspiration difference (kg m^{-2} day^{-1}); swds: Soil moisture storage in the upper layer (kg kg^{-1}); swrz: Soil moisture storage in the root layer (kg kg^{-1}); and swdz: Soil moisture storage in the draining layer (kg kg^{-1}).]

late spring to the summer. However, from fall to early spring, the local sources of moisture supply larger amounts than the external ones (Fig. 6a). Over the southern sector evapotranspiration plays a major role throughout the whole year, and moisture convergence contributes to the maximum of precipitation in early spring (Fig. 6c).

In the land component, the dominance of $P - E$ over runoff values indicates the storage of soil moisture in the area (Figs. 6b,d). Runoff values simulated by CPTEC/COLA represent the sum of direct runoff and baseflow. The baseflow formulation in the model considers the maintenance of a minimum volume during periods of deficits (Sellers et al. 1986). In both sectors, the increase of runoff depends on precipitation excess ($P - E$). During late summer, runoff has similar values to ($P - E$) in the northern sector, and the storage of moisture in the soil is maximum, corresponding to the excess of precipitation (Fig. 6b). During winter, ($P - E$) is negative and the runoff diminishes, although it does not become null, due to the existence of baseflow. Evapotranspiration and minimum runoff are supplied by soil moisture storage (Fig. 6b). In the southern sector, ($P - E$) is maximum in middle autumn and in spring. Runoff and soil moisture storage stay almost constant during the year (Fig. 6d), but they are smaller than in the northern sector (Fig. 6b).

Mean annual values of hydrological variables simulated with CPTEC/COLA and obtained from R2 except for observed precipitation are shown in Table 1 for northern and southern sectors. Simulated precipitation is larger than observed precipitation over the northern sector, simulated evapotranspiration rates are lower than amounts obtained from R2, and ($P - E$) is higher in the CPTEC/COLA simulation. In both, atmospheric ($P - E$ = MFC, where MFC is moisture flux convergence) and land ($P - E$ = Runoff) components, the

TABLE 1. (a) Annual means in (a) northern sector and (b) southern sector (values in mm).

(a)

	NCEP–DOE R2 (CRU/CMAP for P)	CPTEC/COLA ensemble mean	CPTEC/COLA ensemble scatter
$P_{(CRU/CMAP)}$	3.94/3.61	4.23	0.0858
E	3.94	2.66	0.0179
$P - E_{(CRU/CMAP)}$	0.00/0.13	1.57	0.0679
MFC	1.81	1.68	0.0825
Runoff	0.34	1.54	0.0732

(b)

	NCEP–DOE R2 (CRU/CMAP for P)	CPTEC/COLA ensemble mean	CPTEC/COLA ensemble scatter
$P_{(CRU/CMAP)}$	4.01/3.62	2.40	0.0347
E	2.93	2.00	0.0182
$P - E_{(CRU/CMAP)}$	1.08/0.69	0.40	0.0165
MFC	0.36	0.65	0.0267
Runoff	0.213	0.41	0.0244

hydrological unbalance is less than 10% in CPTEC/COLA results. The scatter ensemble of the annual mean, evaluated through the standard deviation of the ensemble members, is low for the hydrological variables (Table 1).

Over the southern sector, the CPTEC/COLA mean annual precipitation is lower than observed precipitation and mean annual evapotranspiration is lower than that obtained from R2 archives. In this case, the hydrological balance of the land component in the model is closer to the equilibrium than that obtained from observed/R2. The atmospheric component of the model has a larger error in this sector than in the northern one.

c. *Boundary fluxes in the two sectors*

In this section, the moisture fluxes integrated vertically and over the lateral boundaries shown in Fig. 1 are calculated for the two sectors. From October to March (warm season) there is a northerly meridional flux in and out of the northern sector. The flux into the northern boundary (15°S) is larger than the flux coming out the southern boundary 25°S into the southern sector (Fig. 7a). The maximum values of meridional flux crossing the northern border are associated with moisture coming from the Amazon region and from the flux turning to south from the Atlantic Ocean (ATL) (Fig. 8a). This is consistent with the fact that in this period there is strong convection and precipitation over the Amazon region, and therefore more moisture is available to be transported southward. In the climatological averages for this period, it is seen that the southward flux has also a component from the ATL that feeds moisture to the northern sector. Similar general features are seen in the R2 field (Fig. 8c).

During the cold season, from April to September, the meridional flux out of the northern sector is larger than the influx into this area (Fig. 7a). The zonal flux in the northern sector is larger than the flux out during the whole year (Fig. 7b). During winter the zonal flux from the ATL produces an accumulation of moisture in the northern sector that is transported meridionally to the southern area, across 25°S (Fig. 7a).

In the southern sector, the meridional moisture flux entering the area from the northern boundary is larger than the meridional flux going out for the whole year with a peak flux that occurs from August to October (Fig. 7c). Taking into account the zonal fluxes, from November to April, water vapor fluxes come from the ATL into the southern sector, but from May to October the flux is reversed and directed from the continent to the ocean (Fig. 7d).

The general spatial and temporal features observed in R2 are well reproduced by CPTEC/COLA, in the tropical South America, that is, the different direction of flux from the Atlantic Ocean over Amazonia in the two different periods of Fig. 8. However, south of 15°S, there are differences related to the flux southward and the LLJ. The flux intensity in the model results is weaker than in the reanalysis, and this is reflected in the underestimated precipitation over the southern sector. In the summer this feature is related to the overestimated flux toward southeastern Brazil that is also associated with overestimation in the SACZ area. Another reason could be errors in the representation of Andes orography, which works as a barrier for the wind flow, forcing the winds southward. Also, analyses of the vertical wind structure and the moisture suggest that errors in the moisture flux are due to the wind fields, rather than to the moisture fields (Wang and Paegle 1996; Rodriguez 2002).

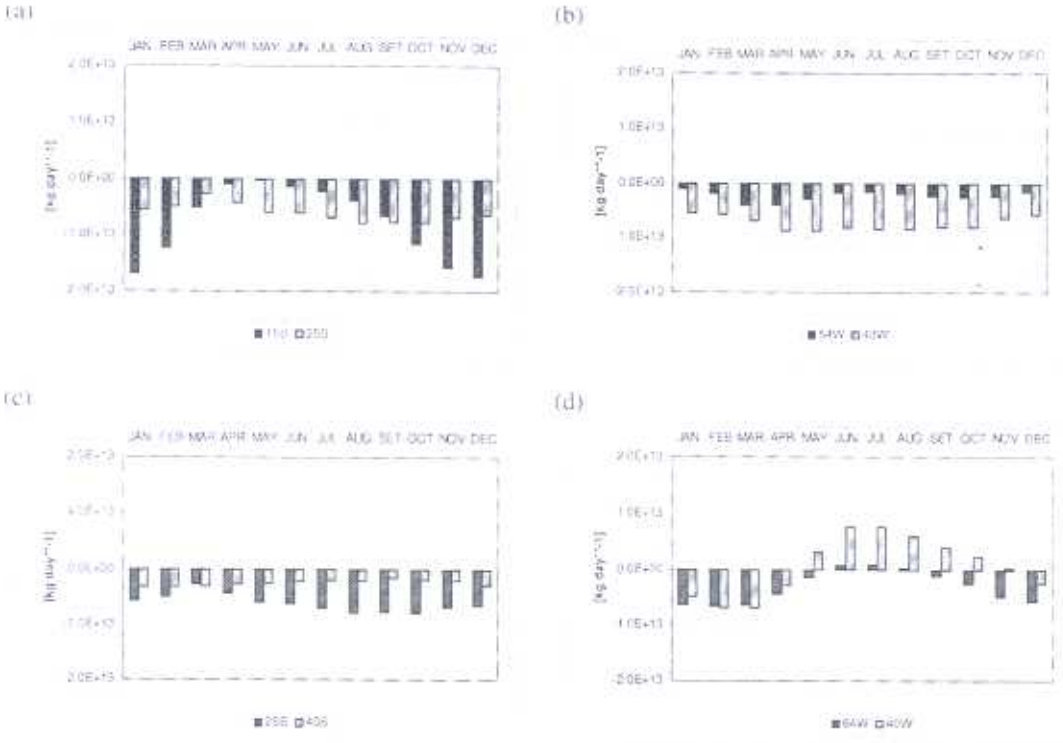

FIG. 7. Moisture flux (kg day $^{-1}$) through the boundaries of the (a), (b) northern and (c), (d) southern sectors at the low levels (surface–850 hPa). Meridional fluxes in (a), (c) and zonal fluxes in (b), (d).

Results show that the main source of moisture to the southern area is provided throughout the year by the northern sector, which receives moisture from the Amazon region and ATL. During winter, larger flux is transferred to the southern sector, crossing 25°S, than the flux that enters the area, and the moisture is supplied by the zonal flux from the Atlantic Ocean. In this season, part of the southern area moisture goes back to the Atlantic Ocean, and in the rest of the months there is an increase of moisture inside the area due to the meridional flux convergence. The meridional flux over central Brazil contributes to the occurrence of maximum moisture convergence in September (Fig. 5d) and maximum precipitation over the southern sector during late spring (Fig. 5c).

Considering that the humidity over the La Plata basin can have contribution of the moisture flux from the ATL and Amazonia, a partition of the flux from three boundaries indicated on Fig. 9 was performed. Only the incoming flux through the boundaries, integrated and divided by the vertical area of the boundaries, was considered. The results show that the flux from the northern boundary is larger than the other boundaries almost during the whole year, with maximum values in the spring and summer seasons. The eastern flux is almost constant during the year, and it is overcome by the flux from the northwest boundary in the summer season. The northwestern flux shows a secondary peak in July, with almost identical magnitude to the eastern fluxes. It is clear that the northern and northwestern fluxes have a major contribution to the moisture in the La Plata region during the summer. During the transition seasons, the moisture is provided from northern and eastern fluxes. In the winter season there is little contribution from all boundaries. The results obtained partitioning the moisture fluxes are consistent with the previous analysis of boundary flux done for the northern and southern sectors.

4. The El Niño 1982/83 and La Niña 1988/89 anomalies

Spring and summer are seasons with a large influence of the LLJ east of Andes on the occurrence of MCC over northern Argentina and Paraguay (Nogués-Paegle et al. 2002). As seen in the previous section, in these seasons there is transport of moisture from the Amazon region and from ATL to the northern sector of SSA. Although the LLJ is well represented by the CPTEC/COLA AGCM with resolution T62L28 (Cavalcanti et al. 2002b), the organized precipitation associated with MCC is not, at this resolution. This inability to simulate

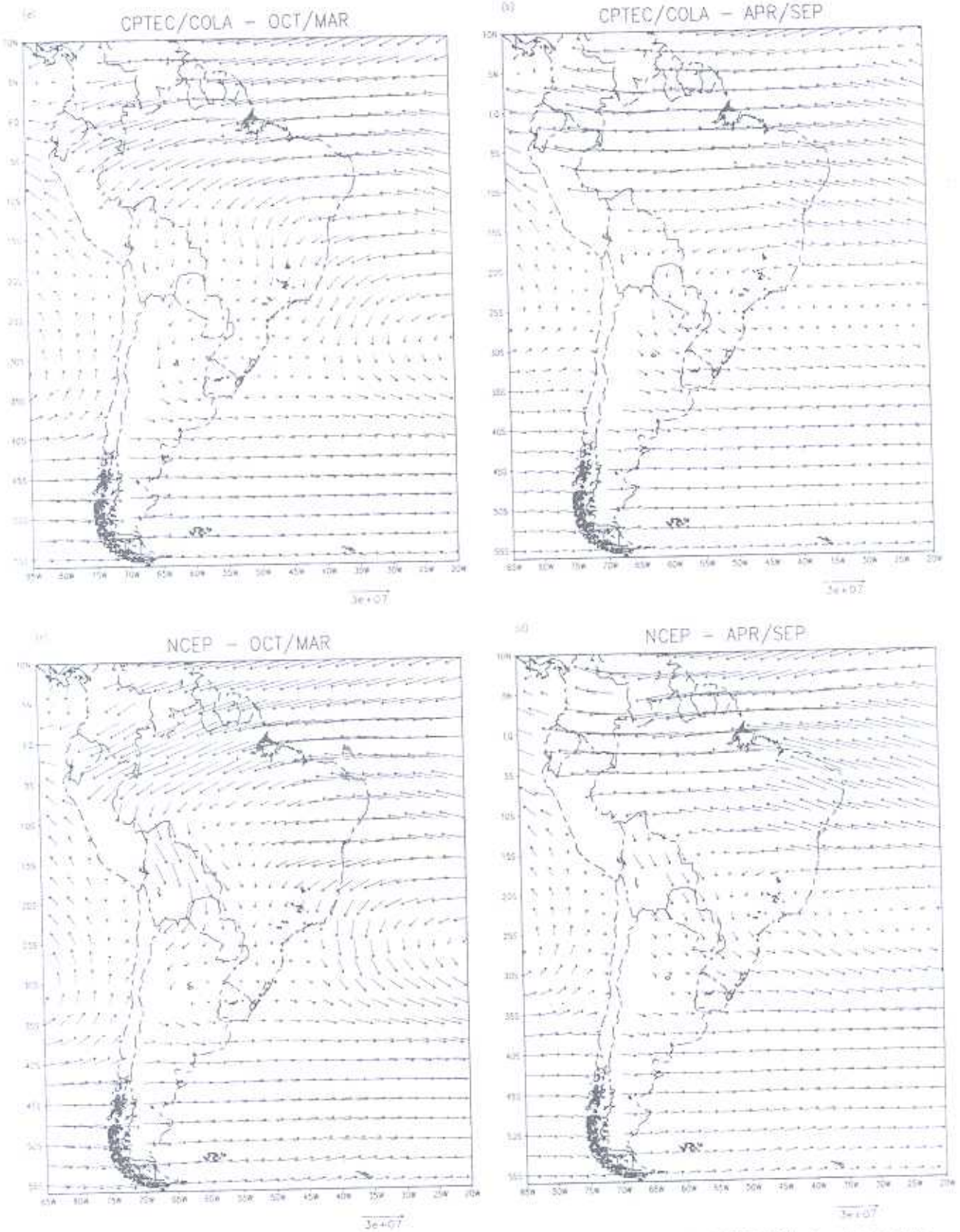

FIG. 8. Climate vertically integrated moisture flux (kg m^{-1} day^{-1}) (surface–300 hPa): (a), (b) CPTEC/COLA and (c), (d) R2.

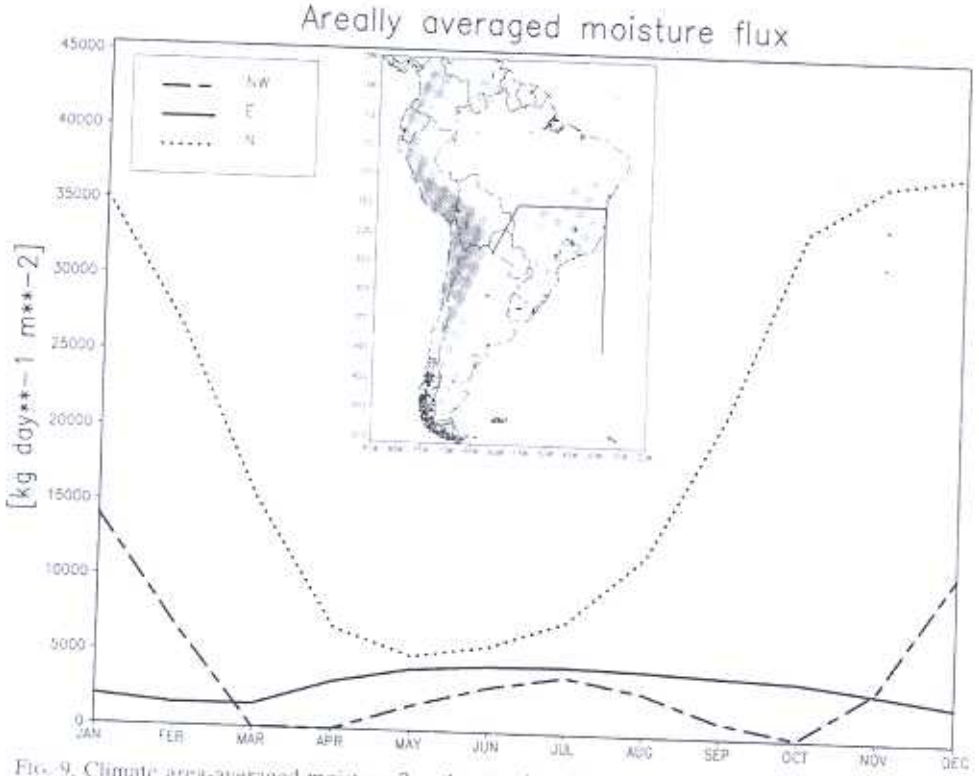

FIG. 9. Climate area-averaged moisture flux (kg day $^{-1}$ m $^{-2}$) through the northwest (23°S, 62°W to 15°S, 58°W), north (15°S, 58°W to 15°S, 35°W), and east (15°S, 35°W to 40°S, 35°W) boundaries.

mesoscale precipitation at this resolution could reduce the simulated convective precipitation over the region, even though the moisture flux transported by the LLJ from the tropical region southward can increase the precipitation in that region, and this feature is simulated by the model. Two examples of opposite ENSO years will be shown, in this section, linking the moisture flux with the precipitation anomalies over the La Plata basin.

To evaluate the skill of CPTEC/COLA in reproducing the components of the hydrological cycle in two extreme climatic conditions, the warm 1982/83 El Niño and the cold 1988/89 La Niña episodes were selected. The spatial averaged precipitation variability from September to February in the two opposite ENSO years is better simulated over the northern sector than over the southern sector for the ensemble mean (Figs. 10a–d), besides the differences between both observed datasets in La Niña summer (Figs. 10b,d). Table 2 shows September–February mean values of the variables from CPTEC/COLA model and R2, and CRU observations for precipitation, for both El Niño 1982/83 and La Niña 1988/89, and for the 10-yr period average. In the northern sector (Table 2a), precipitation, P-E, MFC, and runoff values are smaller during the 1982/83 episode and higher during the 1988/89 episode than the model climatology. In the southern sector (Table 2b), precipitation, MFC, and runoff are larger than the climatology during the El Niño episode and lower during the La Niña episode. In both sectors the ensemble scatters of the variables are larger during the 1982/83 episode than during the 1988/89 episode. Looking at Fig. 10, this feature can be related to the behavior of only one or two members during 1982/83 summer season.

Differences in model estimation between 1982/83 and 1988/89 episodes for the period September–February are shown in Figs. 11a,b. In the northern sector, there is no difference between the spring of 1982 and 1988; however, in December 1982 and January 1983 the values of precipitation, MFC, and runoff are smaller than in the same months of 1988/89. In opposition, from October to January, the southern sector presents higher values of precipitation, MFC, and runoff in the 1982/83 episode than in the 1988/89 episode. Differences in evaporation between these El Niño and La Niña episodes are small in the northern sector, but they become substantially larger in El Niño compared to La Niña for the months of December to February in the southern sector.

The meridional moisture flux in the northern and southern boundaries of the northern sector are larger in 1982/83 than in 1988/89 (Figs. 12a,c); however, the in-

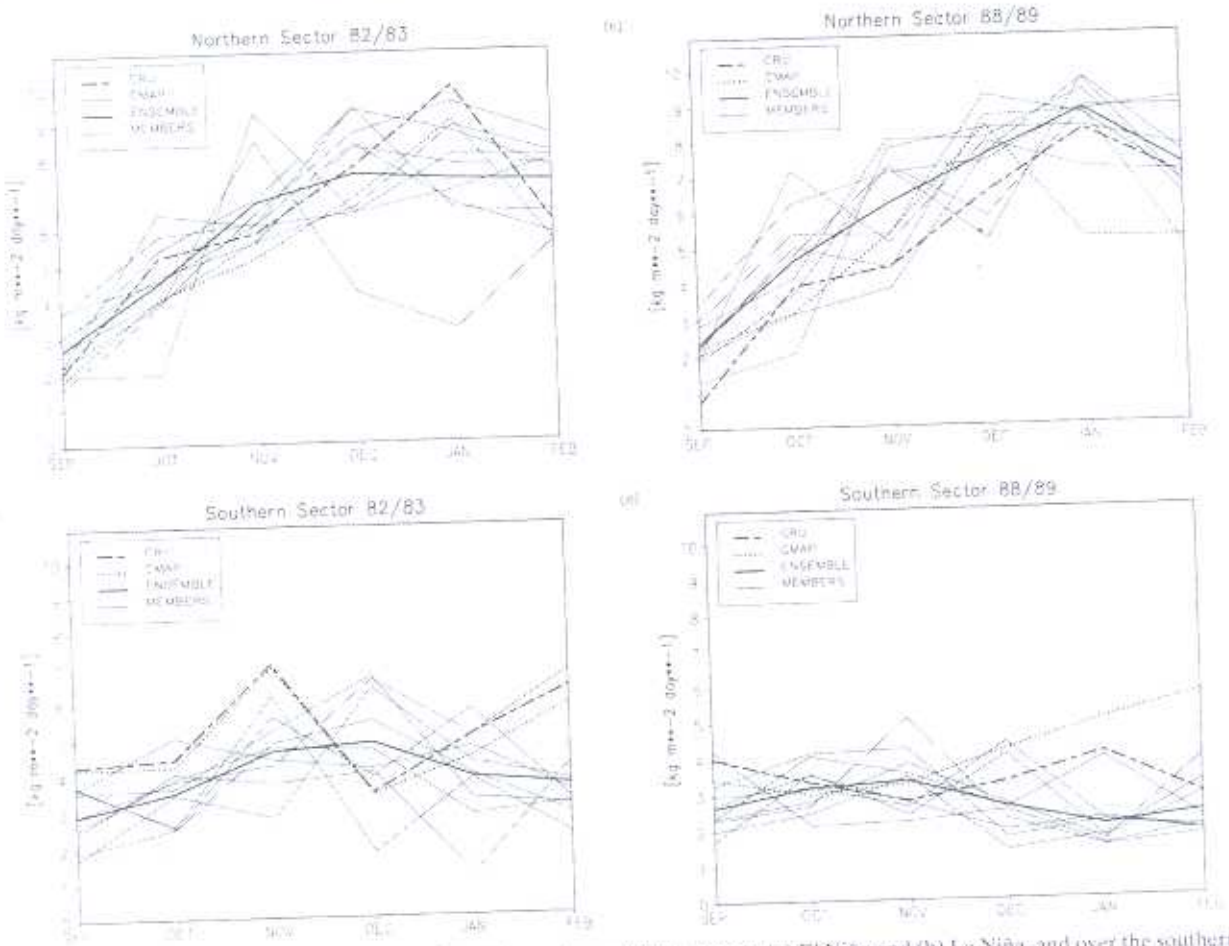

FIG. 10. Spatial averaged precipitation (kg m $^{-2}$ day $^{-1}$) over the northern sector in (a) El Niño and (b) La Niña, and over the southern sector in (c) El Niño and (d) La Niña. CPTEC/COLA ensemble members in solid lines, CPTEC/COLA ensemble average in solid thick line, CMAP precipitation in dotted line, and CRU precipitation and R2 MFC in dashed line.

coming flux exceeds the outgoing flux in both situations in agreement with the climatology. Incoming zonal moisture flux is clearly larger than zonal outgoing flux in the northern sector during both events (Figs. 12b,d). In the southern sector, the incoming meridional flux through the 25°S boundary is larger during the summer season of 1982/83 than that of 1988/89 (Figs. 13a,c). Divergence of zonal moisture flux is evident during the 1982/83 event in the southern sector (Fig. 13b). Therefore, the MFC in this sector during the El Niño episode results mainly from the meridional flux convergence. On the other hand, net moisture flux convergence is found in the southern area during 1988/89 as a result of an augmented zonal flux into the region (Fig. 13d). These results indicate that La Plata basin received moisture from the Amazon region and from ATL in both episodes. However, the moisture flux from the Amazon region was dominant in the 1982/83 episode for both sectors while the ATL is the dominant contributor for the southern sector during the 1988/89 episode.

In addition to the previous analysis, the differences of precipitation, wind, and moisture flux between the two episodes are shown in spatial fields. Because of negligible differences during the spring, the difference fields are only shown for the summer. Precipitation differences between El Niño and La Niña, in this season, are shown in Fig. 14. Extreme opposite precipitation anomalies occurred over SSA during El Niño 1982/83 and La Niña 1988/89. These anomalies indicated an opposite north–south dipole in these two years. Dry conditions over northeast Brazil and excess of precipitation over SSA occurred in 1982/83, and deficit of precipitation over SSA and above-normal rainfall over the northeast occurred in 1988/89. The excess of precipitation over SSA during El Niño compared to La Niña can be related to wind and moisture differences at low levels of the atmosphere (Fig. 15a).

TABLE 2. September–February mean in the (a) northern sector and (b) southern sector (values in mm).

(a)

	CPTEC/COLA climate		CPTEC/COLA 1982/83		CPTEC/COLA 1988/89	
	Ensemble mean	Ensemble scatter	Ensemble mean	Ensemble scatter	Ensemble mean	Ensemble scatter
P	6.34	0.0236	6.20	0.4587	6.50	0.166
E	3.33	0.0014	3.46	0.0148	3.30	0.0283
$P - E$	3.01	0.0222	2.74	0.4439	3.20	0.1377
MFC	3.35	0.02	3.06	0.4212	3.48	0.0833
Runoff	1.95	0.0134	1.57	0.1881	2.17	0.0699

(b)

	CPTEC/COLA climate		CPTEC/COLA 1982/83		CPTEC/COLA 1988/89	
	Ensemble mean	Ensemble scatter	Ensemble mean	Ensemble scatter	Ensemble mean	Ensemble scatter
P	3.05	0.0029	3.91	0.2388	2.69	0.0557
E	2.67	0.0009	3.04	0.0419	2.52	0.0103
$P - E$	0.83	0.002	0.88	0.197	0.17	0.0454
MFC	0.77	0.0019	1.31	0.1537	0.59	0.0499
Runoff	0.48	0.0010	0.74	0.0648	0.39	0.0148

Strong flow from the Atlantic Ocean to the Amazon region and then toward La Plata basin occurred during the 1982/83 episode in contrast to the 1988/89 episode, when the wind flow was significantly weaker. As a result, the influx of water vapor was larger over SSA during the El Niño episode than during the La Niña episode, illustrated by the differences in moisture fluxes between the two episodes (Fig. 15b). As there was deficit of precipitation in the northern/northeastern Brazil in 1982/83, the moisture that normally goes to the atmosphere in the Amazon region was advected southward by the low-level flow.

The vertically integrated moisture flux (Figs. 16a,b) shows that in 1982/83 the water vapor flux was directed from the Atlantic Ocean toward tropical Brazil across the Amazon region and turning southward. On the other hand, in the 1988/89 episode, the flux from the Atlantic Ocean into the Amazon region was weaker than in the 1982/83 episode with a dominance of water vapor toward southeastern Brazil, to the SACZ area.

5. Conclusions

Based on the different precipitation regime of the northern and southern sectors of the La Plata River basin, also shown in Berbery and Barros (2002), the hydrological study was performed separately in the two sectors. The northern sector, which is influenced by the SACZ, presents a well-defined annual cycle and the southern sector has a less marked annual variability,

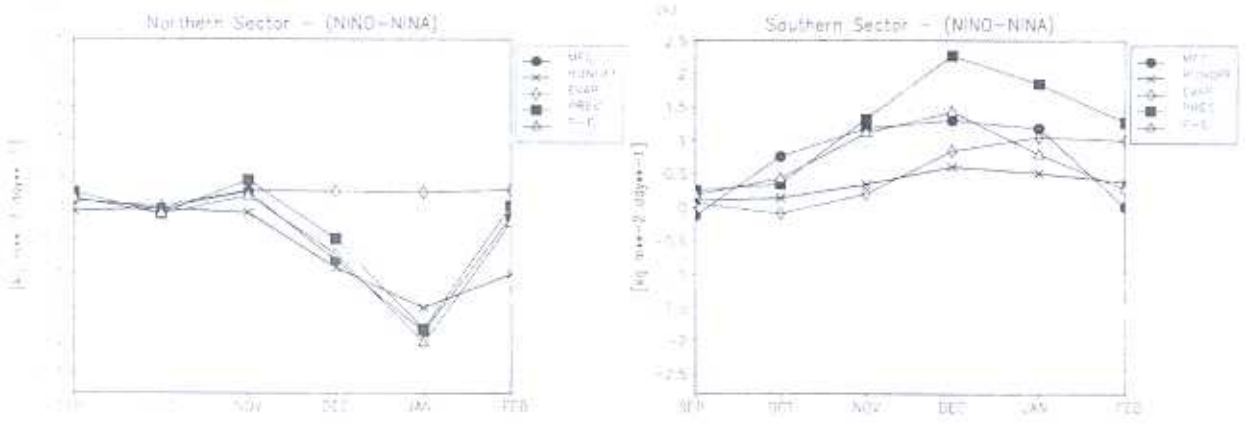

FIG. 11. Differences between the variables in El Niño 1982/83 and La Niña 1988/89 in both (a) northern and (b) southern sectors. [EVAP: Evapotranspiration (kg m^{-2} day^{-1}); PREC: Precipitation (kg m^{-2} day^{-1}); RUNOFF: Runoff (kg m^{-2} day^{-1}); MFC: Vertically integrated (surface–300 hPa) moisture flux convergence (kg m^{-2} day^{-1}); and $P - E$: Precipitation and evapotranspiration difference (kg m^{-2} day^{-1}).]

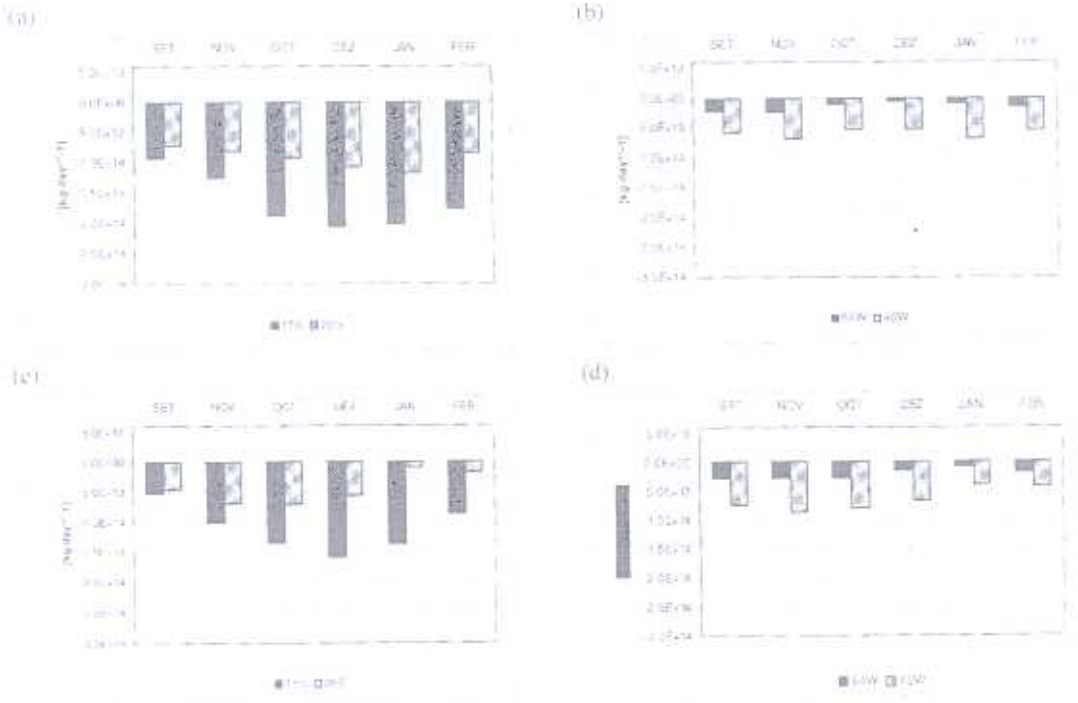

FIG. 12. Moisture flux (kg day^{-1}) through the boundaries at the low levels (surface–850 hPa), in the northern sector: (a), (b) El Niño and (c), (d) La Niña. Meridional fluxes in (a), (c) and zonal fluxes in (b), (d).

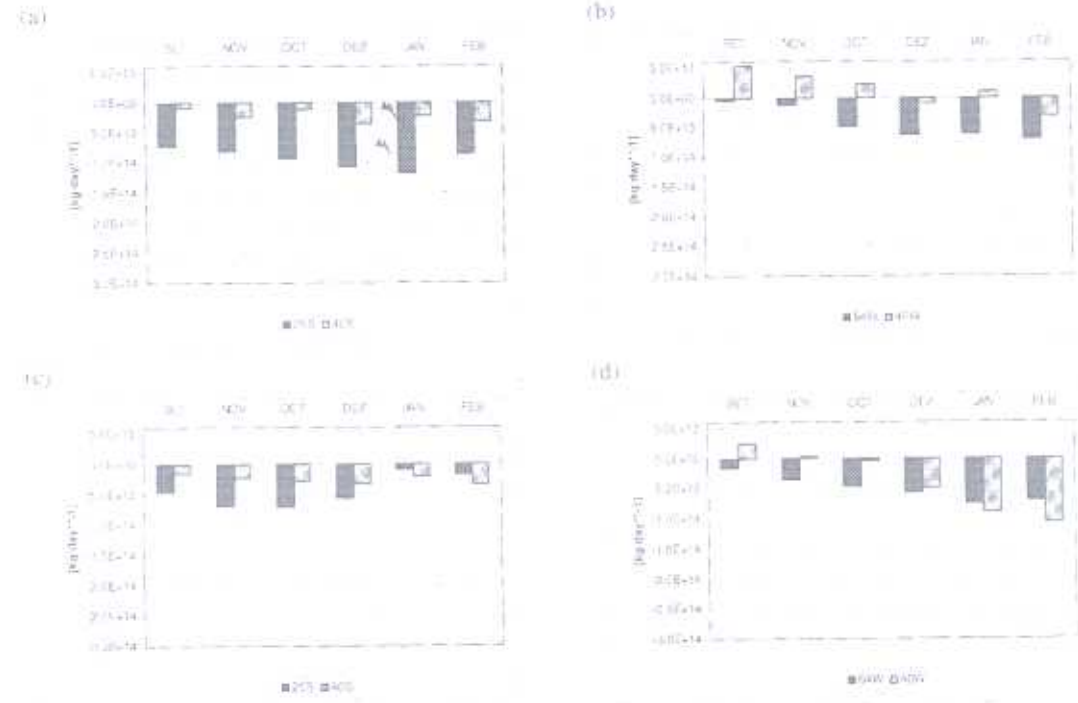

FIG. 13. Moisture flux (kg day^{-1}) through the boundaries at the low levels (surface–850 hPa), in the southern sector: (a), (b) El Niño and (c), (d) La Niña. Meridional fluxes in (a), (c) and zonal fluxes in (b), (d).

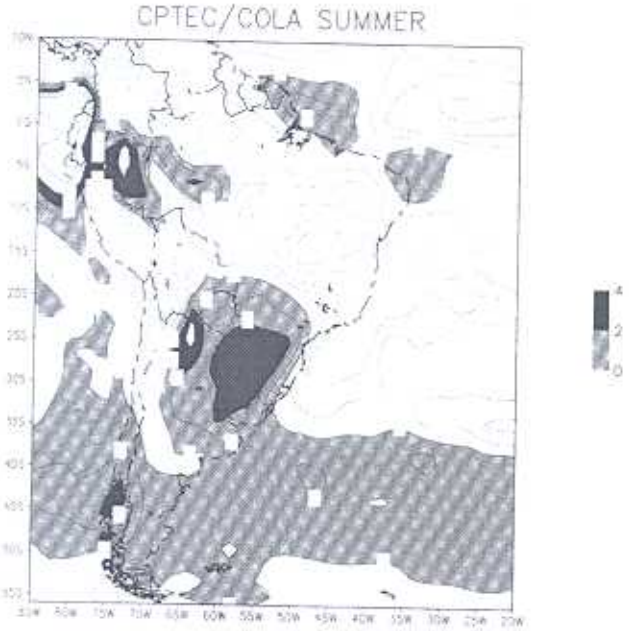

FIG. 14. Differences between summer precipitation (kg m^{-2} day^{-1}) during El Niño 1982/83 and La Niña 1988/89 from CPTEC/COLA AGCM.

features simulated by the model. Over the northern sector the model overestimates both the precipitation and the moisture convergence during summer. During the rest of the year, simulations agree with R2 and observations. In the southern sector, CPTEC/COLA systematically underestimates precipitation and moisture convergence. However, the maximum precipitation in the spring is simulated by the model. The lower values of precipitation simulated by CPTEC/COLA during winter and autumn could be related with less accuracy of the model in simulating the transient components of the flow from higher latitudes and the moisture transported by the low-level flow east of Andes. These processes explain much of the winter precipitation over the southern sector (Vera et al. 2002; Berbery and Barros 2002). The land and atmosphere components of the hydrological cycle of CPTEC/COLA are almost balanced in the annual scale over northern sector. This behavior is shown for the land component in the southern sector too, while the atmospheric component has a large unbalance over this sector.

Climatological analyses show that the wind flow, at low levels, changes over northern and central South America from spring/summer to autumn/winter, affecting the moisture flux to the northern and southern sectors of the La Plata basin. These features are well represented by the model. The moisture sources analyses show that the incoming northwest moisture flux into northern sector is larger than the easterly flux during

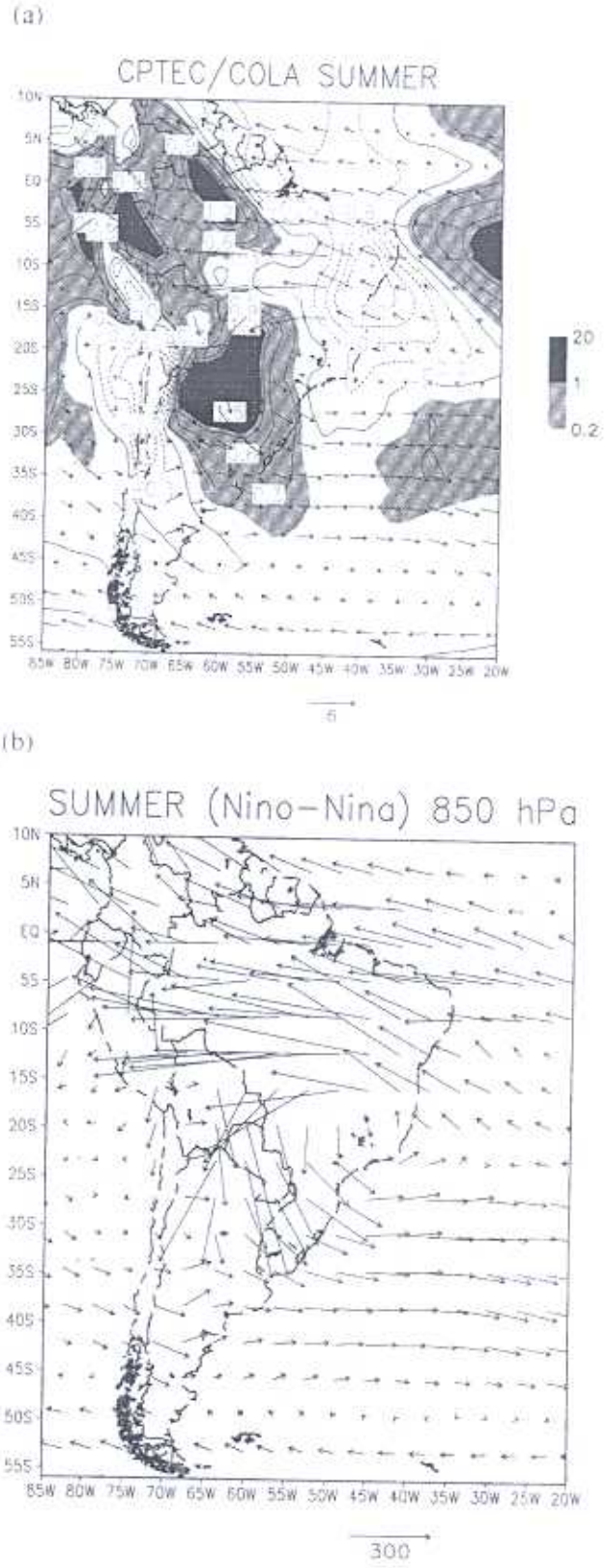

FIG. 15. Summer differences of El Niño 1982/83 and La Niña 1988/89 (a) specific humidity (×1000) at 700 hPa and winds at 850 hPa (m s^{-1}), and (b) moisture flux at 850 hPa (kg m^{-1} day^{-1}) from CPTEC/COLA AGCM.

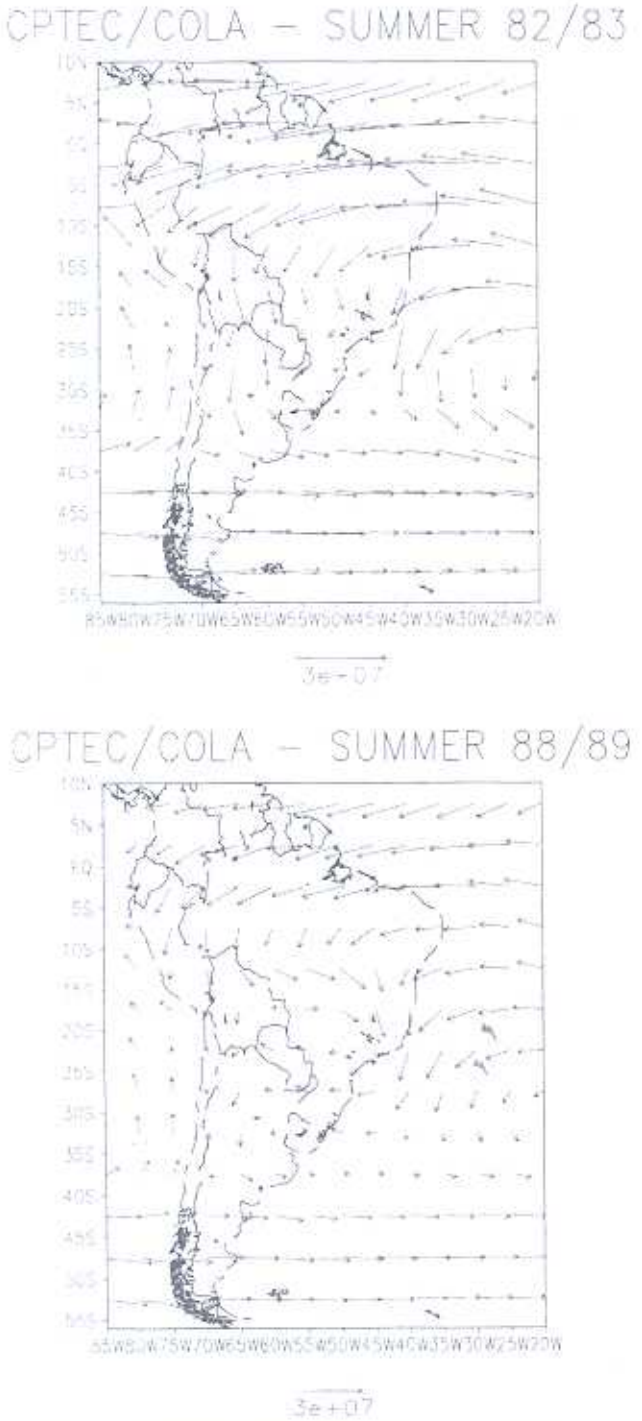

FIG. 16. Vertically integrated moisture flux in summer (a) El Niño 1982/83 and (b) La Niña 1988/89 yr (kg m^{-1} day^{-1}) from CPTEC/COLA AGCM.

late spring and summer, contributing to the moisture of La Plata basin during these months, in addition to the northerly flux contribution. During autumn, winter, and early spring, the moisture flux from ATL. overcomes the incoming northwest flux; however, it is much smaller than the spring and summer northerly flux. In the southern sector, during winter months, external sources of moisture (moisture convergence) supply almost the same quantities than local sources (evaporation), which are the main source of moisture to the sector during the whole year. This feature can be linked to rainfall provided by frontal systems that penetrate into the region throughout the year and provide extra water to the region.

Large precipitation differences between El Niño (1982/83) and La Niña (1988/89) occurred over SSA. During 1982/83, the moisture over the Amazon region was transported southward by the low-level flux whereas during the 1988/89 episode, moisture flux was directed to southeastern Brazil. Analyzing the contributions of the meridional and zonal fluxes to the southern sector, it is seen that in 1988/89 there is a dominance of flux from the ATL compared to the meridional flux from the northern sector. In 1982/83 there was larger meridional moisture flux from the Amazon region to the southern sector than the zonal flux from the subtropical Atlantic. This feature is in agreement with results found by Saulo et al. (2000) for the 1997/98 warm season. The low scatter of the model's members in both climatology and anomalies of two ENSO years indicates a good agreement among the ensemble members. Convergence among members was also shown in Marengo et al. (2003) in analysis of annual cycle precipitation. However, in that study, there was large dispersion when interannual anomalies were discussed for the southeastern region of South America.

Therefore, consistent also with other previous studies of Berbery and Collini (2000) and Saulo et al. (2000), the present results indicate that moisture from the tropical Atlantic Ocean and Amazon region plays an important role in precipitation over the La Plata basin related to its annual cycle and also to anomalies that are responsible for floods or droughts in the region, in the AGCM simulations.

Initially, this study was developed using the NCEP–NCAR reanalysis and then replaced by the reanalysis II of NCEP–DOE, mentioned in section 2. Few differences in MFC fields and in vertically integrated flux over the SSA region were found between the two datasets, at the time scales used in this work. However, the MFC annual mean was higher for R2 than the previous reanalysis, over the northern sector, and lower over the southern sector; R2 showed higher annual mean runoff, over both sectors, than the NCEP–NCAR reanalysis. Additional studies of hydrological balance over the La Plata basin are being planned considering improvements in the model, such as modified physical

parameterizations and more realistic soil moisture and vegetation.

Acknowledgments. We are grateful to Dr. Hugo Berbery for his useful comments, to FAPESP (Project 01/13816), to IAI/CRN055, to CNPq (Brazil), and to the anonymous reviewers for the suggestions. NCEP reanalysis II data were provided by the NOAA–CIRES Climate Diagnostics Center, Boulder, Colorado (http://www.cdc.noaa.gov/).

REFERENCES

Berbery, E. H., and E. A. Collini, 2000: Springtime precipitation and water vapor flux over southeastern South America. *Mon. Wea. Rev.*, **128,** 1328–1346.

——, and V. R. Barros, 2002: The hydrologic cycle of the La Plata basin in South America. *J. Hydrometeor.*, **3,** 630–645.

Berri, G. J., and B. J. Inzunza, 1993: The effect of the low-level jet on the poleward water vapor transport in the central region of South America. *Atmos. Environ.*, **27A,** 335–341.

Betts, A. K., and P. Viterbo, 2000: Hydrological budgets and surface energy balance of seven subbasins of the Mackenzie River from the ECMWF model. *J. Hydrometeor.*, **1,** 47–60.

——, ——, and E. Wood, 1998: Surface energy and water balance for the Arkansas–Red River basin from the ECMWF reanalysis. *J. Climate*, **11,** 2881–2897.

Bonan, G. B., 1998: The Land Surface Climatology of the NCAR Land Surface Model coupled to the NCAR Community Climate Model. *J. Climate*, **11,** 1307–1326.

Cavalcanti, I. F. A., J. A. Marengo, H. Camargo, C. C. Castro, M. B. Sanches, and G. O. Sampaio, 2000: Climate prediction of precipitation for the Nordeste rainy season of MAM 2000. *Experimental Long-Lead Forecast Bulletin*, Vol. 9, No. 1, 49–52. [Available online at http://www.iges.org/ellfb/past.html.]

——, and Coauthors, 2002a: Global climatological features in a simulation using the CPTEC-COLA AGCM. *J. Climate*, **15,** 2965–2988.

——, C. A. Souza, and V. E. Kousky, 2002b: The low level jet east of Andes in the NCEP/NCAR reanalysis and CPTEC/COLA AGCM simulation (in Portuguese). *Proc. XII Congresso Brasileiro de Meteorologia*, Foz do Iguaçu, Parana, Brazil, Brazilian Society of Meteorology, 904–913. [Available from CPTEC/INPE, Rodovia Presidente Dutra Km 40 SPRJ, 12630000, Cachoeira Paulista, Brazil.]

Costa, M. H., and J. A. Foley, 1999: Trends in the hydrological cycle of the Amazon basin. *J. Geophys. Res.*, **104** (D12), 14 189–14 198.

Garcia, N. O., and W. M. Vargas, 1996: The spatial variability of runoff and precipitation in the Rio de la Plata basin. *Hydrol. Sci. J.*, **41,** 279–299.

Harding, R. J., and A. M. Jochum, 1995: Atmospheric and hydrological processes and models at the soil–vegetation-atmosphere interface—Preface. *J. Hydrol.*, **166,** R7–R8.

Kalnay, E., and Coauthors, 1996: The NCEP/NCAR 40-Year Reanalysis Project. *Bull. Amer. Meteor. Soc.*, **77,** 437–471.

Kanamitsu, M., W. Ebisuzaki, J. S. Woollen, S.-K. Yang, J. J. Hnilo, M. Fiorino, and G. L. Potter, 2002: NCEP-DOE AMIP II Reanalysis (R-2). *Bull. Amer. Meteor. Soc.*, **83,** 1631–1643.

Kinter, J. L., III, and Coauthors, 1997: Formulation. Vol. 1, The COLA atmosphere–biosphere general circulation model. Rep. 51, COLA, 46 pp.

——, and Coauthors, 1997: Formulation. Vol. 1, The COLA atmosphere–biosphere general circulation model. Rep. 51, COLA, 46 pp.

Kodama, Y., 1992: Large scale common features of subtropical precipitation zones (the baiu frontal zone, the SPCZ, and the SACZ). Part I: Characteristics of subtropical frontal zones. *J. Meteor. Soc. Japan*, **70,** 813–836.

Kuo, H. L., 1974: Further studies of the parameterization of the influence of cumulus on large scale flow. *J. Atmos. Sci.*, **31,** 1232–1240.

Labraga, J. C., O. Frumento, and M. López, 2000: The atmospheric water vapor cycle in South America and the tropospheric circulation. *J. Climate*, **13,** 1899–1915.

Laing, A. G., and J. M. Fritsch, 2000: The large-scale environments of the global populations of mesoscale convective complexes. *Mon. Wea. Rev.*, **128,** 2756–2776.

Lau, K. M., J. H. Kim, and Y. Sud, 1996: Intercomparison of hydrologic processes in AMIP GCMs. *Bull. Amer. Meteor. Soc.*, **77,** 2209–2227.

Marengo, J. A., J. Tomasella, and C. R. Uvo, 1998: Trends in streamflow and rainfall in tropical South America: Amazonia, eastern Brazil, and northwestern Peru. *J. Geophys. Res.*, **103,** 1775–1783.

——, and Coauthors, 2003: Assessment of regional seasonal rainfall predictability using the CPTEC/COLA atmospheric GCM. *Climate Dyn.*, **21,** 459–475.

New, M., M. Hulme, and P. Jones, 1999: Representing twentieth-century space–time climate variability. Part I: Development of 1961–96 mean monthly climatology. *J. Climate*, **12,** 829–856.

——, ——, and ——, 2000: Representing twentieth-century space–time climate variability. Part II: Development of 1901–96 monthly grids of terrestrial surface climate. *J. Climate*, **13,** 2217–2238.

Nicolini, M., and H. E. Berbery, 2000: Low level jets over the Americas. *CLIVAR Exchanges*, Vol. 5, No. 2, International CLIVAR Project Office, Southampton, United Kingdom, 6–8.

——, C. Saoulo, J. C. Torres, and P. Salio, 2002: Enhanced precipitation over southeastern South America related to strong low-level jet events during austral warm season. *Meteorologica*, **27,** 59–70.

Nogués-Paegle, J. N., and Coauthors, 2002: Progress in Pan American Clivar Research: Understanding the South American monsoon. *Meteorologica*, **27,** 1–30.

O'Kane, J., 1994: Mesoscale hydrology and general circulation models—Preface. *J. Hydrol.*, **155,** R7.

Pan, H.-L., 1990: A simple parameterization of evapotranspiration over land for the NMC medium-range forecast model. *Mon. Wea. Rev.*, **118,** 2500–2512.

Peixoto, J. P., and A. H. Oort, 1992: *Physics of Climate*. American Institute of Physics, 520 pp.

Rao, V. B., I. F. A. Cavalcanti, and K. Hada, 1996: Annual variation of rainfall over Brazil and water vapor characteristics over South America. *J. Geophys. Res.*, **101** (D21), 26 539–26 551.

Rasmusson, E. M., 1967: Atmospheric water vapor transport and the water balance of North America. Part I. Characteristics of the water vapor flux field. *Mon. Wea. Rev.*, **95,** 403–426.

Reynolds, R. W., and T. M. Smith, 1994: Improved global sea sur-

face temperature analyses using optimum interpolation. *J. Climate*, **7**, 929–948.

Roads, J., and A. Betts, 2000: NCEP–NCAR and ECMWF reanalysis surface water and energy budgets for the Mississippi River basin. *J. Hydrometeor.*, **1**, 89–94.

——, S. Chen, A. Guetter, and K. Georgakakos, 1994: Large scale aspects of the United States hydrologic cycle. *Bull. Amer. Meteor. Soc.*, **75**, 1589–1610.

——, M. Kanamitsu, and R. Stewart, 2002: CSE water and energy budgets in the NCEP–DOE reanalysis II. *J. Hydrometeor.*, **3**, 227–248.

Rodriguez, D. A., 2002: Hydrologic budget over southern/southeastern South America simulated by the CPTEC/COLA atmospheric model (in Portuguese). M.Sc. thesis, National Institute of Spatial Research, 201 pp. [Available from CPTEC/INPE, Rodovia Presidente Dutra Km 40 SPRJ, 12630000, Cachoeira Paulista, Brazil.]

Satyamurty, P., C. A. Nobre, and P. L. Silva Dias, 1998: South America. *Meteorology of the Southern Hemisphere*, D. J. F. Karoly and D. J. F. Vincent, Eds., Amer. Meteor. Soc., 119–139.

Saulo, A. C., M. Nicolini, and S. C. Chou, 2000: Model characterization of the South American low-level flow during the 1997–1998 spring summer season. *Climate Dyn.*, **16**, 867–881.

Sellers, P. J., Y. Mintz, Y. C. Sud, and A. Dalcher, 1986: A simple biosphere model (SiB) for use within general circulation models. *J. Atmos. Sci.*, **43**, 505–531.

Velasco, I., and J. M. Fritsch, 1987: Mesoscale convective complexes in the Americas. *J. Geophys. Res.*, **92** (D8), 9591–9613.

Vera, C. S., 2004: Introduction to the South American Low-level Jet Experiment (SALLJEX). *CLIVAR Exchanges*, Vol. 9, No. 1, International CLIVAR Project Office, Southampton, United Kingdom, 3–5.

——, P. K. Vigliarolo, and E. B. Berbery, 2002: Cold season synoptic scale waves over subtropical South America. *Mon. Wea. Rev.*, **130**, 684–699.

Virji, H., 1981: A preliminary study of summertime tropospheric circulation patterns over South America estimated from cloud winds. *Mon. Wea. Rev.*, **109**, 599–610.

Wang, M., and J. Paegle, 1996: Impact of analysis uncertainty upon regional atmospheric moisture flux. *J. Geophys. Res.*, **101**, 7291–7303.

Xie, P., and P. A. Arkin, 1996: Analyses of global monthly precipitation using gauge observations, satellite estimates, and numerical model predictions. *J. Climate*, **9**, 840–858.

——, and ——, 1997: Global precipitation: A 17-year monthly analysis based on gauge observations, satellite estimates, and numerical model outputs. *Bull. Amer. Meteor. Soc.*, **78**, 2539–2558.

Xue, Y., P. J. Sellers, J. L. Kinter III, and J. Shukla, 1991: A simplified biosphere model for global climate studies. *J. Climate*, **4**, 345–364.

Zeng, N., 1999: Seasonal cycle and interannual variability in the Amazon hydrologic cycle. *J. Geophys. Res.*, **104** (D8), 9097–9106.